Magnetism from the Atom to the Bulk in Iron, Cobalt, and Nickel Clusters

Isabelle M. L. Billas, A. Châtelain, Walt A. de Heer*

Molecular beam deflection measurements of small iron, cobalt, and nickel clusters show how magnetism develops as the cluster size is increased from several tens to several hundreds of atoms for temperatures between 80 and 1000 K. Ferromagnetism occurs even for the smallest sizes: for clusters with fewer than about 30 atoms the magnetic moments are atomlike; as the size is increased up to 700 atoms, the magnetic moments approach the bulk limit, with oscillations probably caused by surface-induced spin-density waves. The trends are explained in a magnetic shell model. A crystallographic phase transition from high moment to low moment in iron clusters has also been identified.

Ferromagnetism in the transition metals, known since antiquity, is arguably the most intensively studied property of bulk matter. However, several of the most basic questions remain unanswered. For example, the exact nature of the atomic magnetic moments and how they mutually couple to produce macroscopic magnetism are questions that have been debated for decades (*1*). A better understanding of magnetism, especially in small particles (*2*), is crucial not only for basic physics but also because of the great technological importance of ferromagnets for both the recording industry and the emerging nanotechnologies (*3*). Our experiments relate directly to several outstanding questions in magnetism.

The magnetic moment and its temperature dependence are perhaps the most significant physical properties of a ferromagnet (*1*, *4*). We measured these parameters for Fe, Ni, and Co clusters in a molecular beam. The methods used in our molecular beam experiments, which differ from the traditional methods on matrix-supported particles (*5*), offer several important advantages. Molecular beam methods (*6*) allow nearly perfect mass selection of the particles. The interaction-free environment of the molecular beam together with size specificity allow accurate determinations of the intrinsic magnetic moment over wide temperature ranges. However, before discussing the results we briefly review some basic magnetic concepts.

Although a quantitative account of bulk ferromagnetism is involved (*1*, *4*), the basic principles are easily grasped and perhaps best described if we start with the atom and then consider how its properties change in forming the bulk. Atoms of Fe, Co, and Ni have, respectively, 8, 9, and 10 valence electrons distributed in 3*d* and 4*s* levels. Hunds rules (*4*) require that the spin is maximized, so that there are five electrons in the 3*d* spin-up levels, two occupying the 4*s* levels, and the rest in the 3*d* spin-down levels. Hence, the atoms have nonzero spin. Because the magnetic moment of an electron is 1 Bohr magneton, μ_B, the atoms have a magnetic moment.

When the metal atoms come close together, the discrete localized atomic orbitals delocalize, causing cohesion of the atoms, and the discrete atomic levels disperse in energy, giving rise to energy bands (*4*). In the bulk each atom contributes (essentially) one electron to the 4*s* band (in contrast to the atom) (*7*). Nevertheless, the 3*d* electrons remain reasonably localized and retain much of their atomic character. As an approximation, we assume that the 3*d* orbitals do not delocalize at all and hence are atomlike. In that case from Hunds rules the 3*d* spin-up band (called the majority band) is fully occupied (with five electrons per atom) and Fe has two, Co has three, and Ni has four spin-down (minority) electrons per atom. The spin imbalance is simply the difference in the number of spin-up and spin-down 3*d* electrons per atom: $n(+) - n(-)$. Consequently, the magnetic moment (μ) per atom for Fe = $3\mu_B$, for Co = $2\mu_B$, and for Ni = $1\mu_B$. Below we show that these values in fact are quite close to those of very small clusters. The experimental bulk values are $\mu_{Fe} = 2.2\mu_B$, $\mu_{Co} = 1.7\mu_B$, and $\mu_{Ni} = 0.6\mu_B$ (*4*, *8*).

The characteristic noninteger magnetic moments are a consequence of partial delocalization of the 3*d* electrons (which not only enhances the cohesive energy but also contributes to the mutual alignment of the magnetic moments) (*1*). As a result, the magnetic moments are not entirely localized on the atomic cores. Nevertheless, both the local moment approximation [Heisenberg model (*4*)] and the itinerant electron model [Stoner (*1*)] of ferromagnetism have been developed and have their merits and defects. However, the Heisenberg model is particularly well suited to explain the thermal properties.

In addition to what can be learned from the ground state, much information can be obtained from the temperature dependence of the average magnetic moment. At the Curie temperature, T_C, ferromagnetism vanishes. According to the Heisenberg model, this is caused by thermal disorder induced in the mutual alignment of the local magnetic moments, which themselves are relatively insensitive to temperature. However, at and above T_C the average magnetic moment of the whole system vanishes (*4*).

For clusters, the bulk picture is inadequate because a large fraction of the atoms are on the surface where the electronic structure is different from what it is in the bulk. This is partly due to the reduced number of nearest neighbors, which causes the 3*d* electrons to be more localized (*9*). Furthermore, the rather abrupt termination at the surface causes quantum mechanical electronic shock waves to propagate into the cluster, in the form of spatially oscillating charge- and spin-density waves. These waves are known as Friedel (*4*) or RKKY (*10*) oscillations, and they affect the magnetic moment.

One can determine the magnetic moments of clusters by measuring their deflections in an inhomogeneous magnetic field (*11*, *12*) (Fig. 1). A beam of neutral clusters produced in a variable temperature laser vaporization cluster source (*12*) is collimated with 0.8-mm slits and passes between the pole faces of a Stern-Gerlach magnet ($0 \leq H \leq 7$ kG) located about 150 cm downstream from the source. The clusters are photoionized about 100 cm further downstream, by the sweeping of collimated light from an Ar-F excimer laser across the beam, after which the ionized clusters are detected with a time-of-flight mass spectrometer (*13*). A time window on the detector counting electronics selects cluster ions within the corresponding mass range. Hence, the cluster deflections are measured as a function of size, temperature, and magnetic field strength, from which the magnetic moments are determined (*12*).

Figure 2 shows $\bar{\mu}$ in units of μ_B as a function of size for clusters of the three elements at low temperatures. Here $\bar{\mu}$ is the average magnetic moment per atom, which

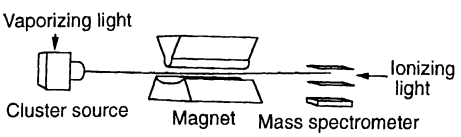

Fig. 1. Schematic diagram of the molecular beam apparatus. A beam of metal clusters is created with the variable temperature laser vaporization source and is deflected with a Stern-Gerlach magnet. Deflections of size-selected clusters are measured with a time-of-flight mass spectrometer.

Institut de Physique Expérimentale, Ecole Polytechnique Fédérale Lausanne, PHB Ecublens, CH-1015, Lausanne, Switzerland.

*To whom correspondence should be addressed.

is formally identical to the (more commonly used) saturation magnetization per atom. Also shown is the average imbalance of the electronic spin populations in the cluster: $n(+) - n(-) = 2\,\overline{\mu}/gx$, where gx is the bulk g factor (*14*): $g_{Fe} = 2.09$, $g_{Co} = 2.25$, $g_{Ni} = 2.18$ (for a free electron $g = 2.00$; shifts are caused by orbital effects). It is striking that in all three cases, for small clusters, the spin imbalances are very close to the values estimated in the atom-based localized moment picture and that for larger clusters the spin imbalances decrease to their bulk limits.

Nickel clusters converge to the bulk limit more rapidly than Co and Fe clusters. In particular, the moment of a Ni cluster with about three layers of atoms (Ni_{150}) is bulklike, whereas for Co and Fe about four to five layers are required (Co_{450}, Fe_{550}) before the same bulklike behaviors are observed. This can be interpreted as indicating how deep into the cluster the perturbations caused by the surface penetrate into the cluster.

More quantitatively, using a magnetic shell model where the magnetic moment of an atom depends on how far below the surface it is located, that is, on its layer index number independent of the size of the cluster, we assign values (μ_1, μ_2, μ_3, and so on) to indicate the magnetic moment (in units of μ_B) of the atoms in layers 1, 2, 3, and so on, where layer 1 indicates the surface. Rough agreement with experiment is obtained by assigning for Ni: (1.15, 0.0, 0.6, 0.4, 0.6, 0.6, 0.6, and so on), for Co: (2.5, 0.7, 2.5, 2.1, 1.7, 1.7, 1.7, and so on), and for Fe: (3.0, 2.8, 2.0, −1.5, 2.0, 2, 2, 2.2, and so on) in units of μ_B. Hence, the observed decreasing trends are reproduced, but not the fine structure. This *aufbau* picture suggests that the surface atoms are atomlike and deep layers are bulklike.

The moments oscillate, and the period for Ni and Co is about one atomic layer. We find that for Ni the second layer is magnetically "dead," and for Fe it appears that the fourth layer is antiferromagnetically coupled. Because the model is rather crude, these assignments are only suggestive. For example, streric effects, which we ignore, are certainly important. Nevertheless, enhanced surface magnetism has been predicted and observed (*15–18*). Furthermore, surface-induced Friedel-type oscillations in the spin density have also been predicted in some calculations (*2*, *15*, *16*). The increasing valence electron densities from Fe to Ni result in progressively more efficient screen-

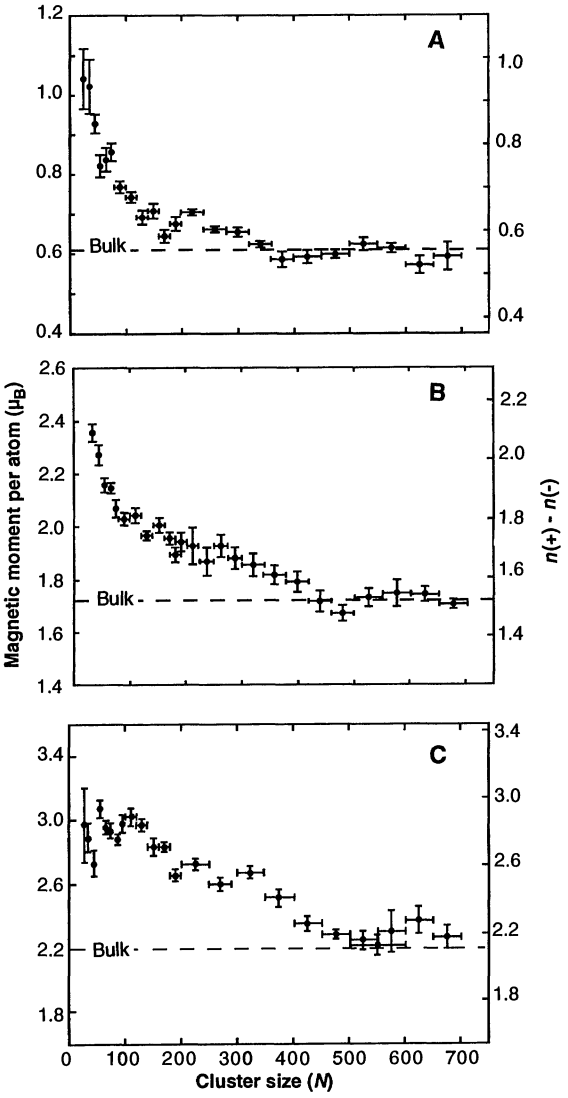

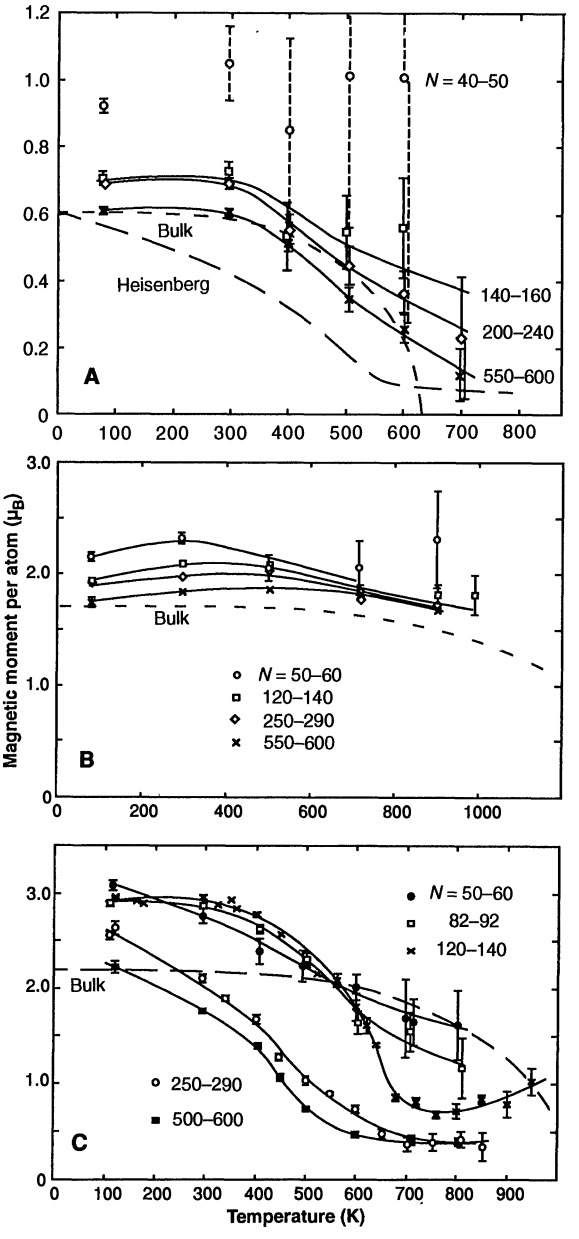

Fig. 2 (right). Low-temperature average magnetic moments ($\overline{\mu}$) per atom for (**A**) Ni clusters at 78 K, (**B**) Co clusters at 78 K, and (**C**) Fe clusters at 120 K, as a function of the number of atoms in the clusters N, showing the evolution to the bulk. The right scale gives the spin imbalance per atom. Very small clusters have large magnetic moments, consistent with localized, more atomic-like moments. The decrease is explained in a shell model where the magnetic moment of an atom in the cluster depends on its distance from the surface, the surface atoms having larger moments than atoms in deeper layers. Superimposed oscillations are probably caused by spin-wave structures. **Fig. 3 (far right).** Average magnetic moments as a function of temperature for several cluster size ranges. Absent error bars indicate that the errors are within the symbol size, and solid lines are guides to the eye. For smaller Ni and Co clusters the average magnetic moments are larger than for the bulk over the measured temperature range, indicating a strong ferromagnetic coupling. Nickel clusters (**A**) show a gradual convergence to the bulk, approximately attained for $Ni_{500-600}$. A slight initial increase is observed in Co clusters (**B**). The anomalous behavior of Fe clusters (**C**) is most likely related to a crystal-phase transition where the transition temperature decreases with increasing cluster size.

ing of perturbations. This could partly account for the more rapid convergence to bulk for Ni clusters than for Co and Fe clusters (*15*). Furthermore, we suspect that spin-wave structures are also responsible for the weak superimposed oscillations; however, our model is too crude to reveal these details.

The ferromagnetic state not only requires (quasilocal) magnetic moments but also requires that the moments remain mutually aligned even at relatively high temperatures (because of the strong interatomic exchange interaction, characteristic for ferromagnets) (*1*, *4*). Temperature-dependent measurement of $\bar{\mu}$ in Fig. 3 show that this is indeed the case even for the smallest clusters. For example, the bulk $\bar{\mu}$ for Ni clusters is practically constant up to 300 K and decreases at higher temperatures, which indicates that for them the interaction affecting the mutual alignment is on the same order as in the bulk. Also the $Ni_{550-600}$ data are already quite bulklike, apart from the smoother transition near T_C. The latter is a characteristic small particle effect (*19*) [found qualitatively in Heisenberg model calculations (*20*) shown in Fig. 3]. Similar conclusions can be drawn for Co clusters; however, $\bar{\mu}$ increases slightly with increasing T. This could be related to a smaller ($\approx$1.5%) increase observed in the bulk at 650 K where it is caused by the phase transition from hexagonal close-packed to face-centered-cubic (*21*).

Compared with Ni and Co clusters, Fe clusters are clearly anomalous. Anomalies in Fe clusters may be expected because, for Fe, in contrast with Ni and Co, the magnetic moment is very sensitive to its environment: changes in the crystal structure strongly affect the magnetic moment (*1*, *17*). For $Fe_{120-140}$ near 600 K, one observes a rather pronounced decrease in $\bar{\mu}$ from about $3\mu_B$ to about $0.6\mu_B$. Larger clusters have high-temperature moments of about $0.4\mu_B$. These effects most likely reflect related behavior in the bulk where the low-temperature, body-centered-cubic phase with $\bar{\mu} = 2.2\mu_B$ transforms into a low moment face-centered-cubic phase at $T = 1150$ K (that is, above $T_C = 1043$ K) (*8*). Apparently, in Fe clusters this phase transition occurs at progressively lower temperatures as the cluster size is increased. Clearly this trend must reverse for sizes larger than measured here to correspond with the bulk.

In conclusion, our molecular beam measurements on ferromagnetic clusters show the evolution of ferromagnetism from the atom to the bulk. The development occurs gradually and appears to be dominated primarily by electronic effects caused by the surface, which affect the magnetic moments of atoms rather deep inside the clusters. The Heisenberg model calculations poorly reproduce the experimental data in Fig. 3A, because in those calculations only nearest neighbor interactions are taken into account and the local magnetic moments are independent of their location in the cluster. For Ni and Co clusters we essentially traced the evolution from atom to the bulk. However, the transition temperature to the low moment phase of Fe clusters continues to decrease. Further study is required to better understand this transition and how it converges to its bulk limit.

REFERENCES AND NOTES

1. D. C. Mattis, *The Theory of Magnetism* (Springer-Verlag, Berlin, ed. 2, 1988); C. Herring, in *Magnetism*, vol. 4, G. T. Rado and H. Suhl, Eds. (Academic Press, New York, 1966).
2. J. Dorantes-Davila, H. Dreyssé, G. Pastor, *Phys. Rev. B* **46**, 10432 (1992); M. R. Press, F. Liu, S. N. Khanna, P. Jena, *ibid.* **40**, 399 (1989); C. Y. Yang, K. H. Johnson, D. R. Salahub, J. Kasper, R. P. Messmer, *ibid.* **24**, 5673 (1981); K. Lee, K. Callaway, K. Kwong, R. Tang, A. Ziegler, *ibid.* **31**, 1796 (1985).
3. A. J. Freeman, C. Li, R. Q. Wu, in *Science and Technology of Nanostructured Magnetic Materials*, G. C. Hadjipanayis and G. A. Prinz, Eds. (NATO Advanced Study Institutes, Series B, vol. 259, Plenum, New York, 1991), pp. 1–13.
4. N. W. Ashcroft and N. D. Mermin, *Solid State Physics* (Holt, Rinehart & Winston, New York, 1976); C. Kittel, *Introduction to Solid State Physics* (Wiley, New York, 1976).
5. K. Haneda, Z. X. Zhou, A. H. Morrish, T. Majima, T. Miyahara, *Phys. Rev. B* **46**, 13832 (1992), and references therein.
6. For a review of cluster beam methods, see W. A. de Heer, *Rev. Mod. Phys.* **65**, 611 (1993).
7. D. A. Papaconstantanopoulos, in *Handbook of the Band Structure of Elemental Solids* (Plenum, New York, 1986), p. 73.
8. M. B. Stearns, in *Magnetische Eigenschaften von Metallen*, Landolt and Börnstein, Eds. (Springer-Verlag, Berlin, 1986), New Series III/19a, p. 24.
9. A. J. Freeman, C. L. Fu, S. Ohnish, M. Weinert, in *Polarized Electrons in Surface Physics*, R. Feder, Ed. (World Scientific, Singapore, 1985), pp. 3–66.
10. M. B. Stearns, *Phys. Rev. B* **4**, 4081 (1971), and references therein.
11. W. A. de Heer, P. Milani, A. Chatelain, *Phys. Rev. Lett.* **65**, 488 (1990); J. P. Bucher, D. C. Douglass, L. A. Bloomfield, *ibid.* **66**, 3052 (1991).
12. I. M. L. Billas, J. A. Becker, A. Chatelain, W. A. de Heer, *ibid.* **71**, 4067 (1993).
13. P. Milani and W. A. de Heer, *Rev. Sci. Instrum.* **61**, 1835 (1990); W. A. de Heer and P. Milani, *ibid.* **62**, 670 (1991).
14. V. A. Gubanov, A. I. Liechenstein, A. V. Postnikov, *Magnetism and Electronic Structure of Crystals* (Springer-Verlag, Berlin, 1992), p. 79.
15. O. Erikson, A. M. Boring, R. C. Albers, G. W. Fernando, B. R. Cooper, *Phys. Rev. B* **45**, 2868 (1992), and references therein.
16. E. Wimmer, A. J. Freeman, K. Krakauer, *ibid.* **30**, 3113 (1984).
17. R. Wu and A. J. Freeman, *ibid.* **47**, 3904 (1993), and references therein.
18. C. S. Wang and A. J. Freeman, *ibid.* **24**, 4364 (1981).
19. Y. Imry, *ibid.* **21**, 2042 (1980); M. E. Fisher and A. N. Berker, *ibid.* **26**, 2507 (1982).
20. K. Binder, H. Rauch, V. Wildpaner, *J. Phys. Chem. Solids* **31**, 391 (1990).
21. E. P. Wohlfarth, in *Ferromagnetic Materials*, E. P. Wohlfarth, Ed. (North-Holland, New York, 1980), vol. 1, pp. 3–70; H. P. Myers and W. Sucksmith, *Proc. R. Soc. London Ser. A* **207**, 427 (1951); M. Pellarin *et al.*, *Chem. Phys. Lett.* **217**, 349 (1994).

22. We thank P. Ballone for continued interest and valuable suggestions. This research is supported by the Swiss National Fund.

19 May 1994; accepted 26 July 1994

All-Polymer Field-Effect Transistor Realized by Printing Techniques

Francis Garnier,* Ryad Hajlaoui, Abderrahim Yassar, Pratima Srivastava

A field-effect transistor has been fabricated from polymer materials by printing techniques. The device characteristics, which show high current output, are insensitive to mechanical treatments such as bending or twisting. This all-organic flexible device, realized with mild techniques, opens the way for large-area, low-cost plastic electronics.

Organic semiconducting materials, such as conjugated polymers and oligomers, have recently been used as active layers in electronic devices, such as field-effect transistors (FETs) (*1*) and electroluminescent diodes (LEDs) (*2*). By a further use of organic compounds as substrates or contact electrodes, "all-organic" devices were developed first for FETs (*3*) and later for LEDs (*4*), thereby creating the promising perspective of low-cost and large-area fabrication of flexible devices. However, the term all-organic is in its strictest sense misleading because the reported structures still contain a metallic part, the gold source and drain electrodes in FETs or the rectifying calcium or magnesium electrode in LEDs. The deposition process of these electrodes, requiring high vacuum and temperature, creates a constraining costly step in the device fabrication. Furthermore, these metal-organic interfaces, which cannot be considered as fully flexible, form a potential source of mechanical and chemical instability. We report here a fully organic device, an all-polymer FET fabricated solely by printing techniques, which opens the field of flexible plastics electronics.

Laboratoire des Matériaux Moléculaires, CNRS, 2 rue Dunant, 94320 Thiais, France.

*To whom correspondence should be addressed.